Semiconductor Physics, Quantum Electronics & Optoelectronics, 2025. V. 28, No 2. P. 175-182.

Hetero- and low-dimensional structures

Dielectric losses in SiO_x&Fe_yO_z(Fe) nanocomposite films

A.A. Evtukh[1,2], S.V. Antonin[1], A.I. Pylypov[2], O.L. Bratus[1]

[1]V. Lashkaryov Institute of Semiconductor Physics, NAS of Ukraine, 41 Nauky Ave., 03028 Kyiv, Ukraine
[2]Educational and Scientific Institute of High Technologies, Taras Shevchenko National University of Kyiv, 64, Volodymyrska Street, 01601 Kyiv, Ukraine
[*]Corresponding author: e-mail: antoninsv@gmail.com

Abstract. Studies of the dielectric behavior of nanocomposite films are critical for a better understanding of electromagnetic wave absorption. This work presents results on investigating dielectric losses in nanocomposite SiO_x&Fe_yO_z(Fe) films. The films with different compositions were obtained using the physical ion-plasma sputtering method. The dielectric losses have been studied within the frequency range of 5 kHz…5 MHz. The decrease of the dielectric losses of the applied signal with the frequency and their increase with the voltage have been demonstrated. The content of SiO_x&Fe_yO_z(Fe) nanocomposite films and high-temperature annealing significantly influence the dielectric losses. The highest dielectric losses have been observed for the initial Fe_yO_z films. In the case of annealed films, the highest dielectric losses were observed when the ratio Fe:Si of iron and silicon areas of the sputtering target were equal to 1:2 and 1:1. The ascertained results have been explained using the phenomenon of space charge polarization in phase interfaces.

Keywords: nanocomposite films, dielectric losses, polarization, frequency, voltage, ion-plasma deposition, annealing.

https://doi.org/10.15407/spqeo28.02.175
PACS 62.25.De, 73.61.-r, 77.22.Gm, 81.07.-b, 81.15.-z

Manuscript received 12.03.25; revised version received 08.05.25; accepted for publication 11.06.25; published online 26.06.25.

1. Introduction

Dielectric materials are widely used in various applications. The specific capacitance and dielectric losses are among the most important parameters of the capacitors. Applying dielectrics in mm-wave detectors, the dielectric losses limit the overall optical efficiency when transferring the received mm-wave signal from the antenna to the detectors [1]. The dielectric losses are also critical for on-chip spectroscopy, where they constrain the quality factor [2]. Nowadays, these dielectrics with low losses, namely SiO_2 [3], SiN_x [4, 5], amorphous Si [6] and silicon carbide [7], are widely used. This low-loss tangent (10^{-5}) has been observed for a-Si [6] and silicon carbide [7] at microwave frequencies.

On the other hand, the dielectrics with high dielectric constant and low losses are very attractive for use as supercapacitors. The composites containing metal and silicon nanoparticles in the dielectric matrix are under intensive investigations [8–13]. Giant dielectric constant values (~10^{10}) have been obtained for the composite film copper nanowires/amorphous SiO_2 [14]. Some composite materials demonstrate the appearance of negative capacitance [15–17]. This unusual effect is promising for using the composite materials in novel micro- and nanoelectronics devices.

On the contrary, when using nanocomposite materials as an absorber of electromagnetic waves, the higher the dielectric loss, the better. The most important properties of the primary material that achieves electromagnetic absorption are the imaginary parts of complex permittivity $\varepsilon_r = \varepsilon' - j\varepsilon''$, complex permeability $\mu_r = \mu' - j\mu''$, and complex conductivity $\sigma_r = \sigma' - j\sigma''$, but there are no materials that give high values for all of these parameters at all frequencies. The higher the values of ε, the higher the attenuation constant, and the attenuation of the electromagnetic wave will be stronger [18–20]. Nowadays, a variety of microwave absorption materials are under intensive investigation, aiming to create an effective microwave absorber. Among microwave absorption materials, the ferrites, namely ferrospinels and hexaferrites, attract significant research interest owing to their high magnetic loss and large Snoek's limit [21–23]. To date, many ferrite microwave absorbers have been developed, including $ZnFe_2O_4$, $BaFe_{12-x}Al_xO_{19}$ (x = 0.1…1.2), and $Ce(FeTi)O_x$, which hold significant potential in the microwave absorption domain due to their remarkable magnetic and dielectric properties. Furthermore, researchers discovered that cation substitution can affect magnetic characteristics and microwave absorption performance of ferrite microwave absorbers [24, 25].

This work presents the results of an investigation of dielectric losses of alternating electrical signals in nanocomposite $SiO_x\&Fe_yO_z(Fe)$ films depending on their content.

2. Experimental

Nanocomposite films were prepared using the ion plasma deposition [26, 27]. The combined target containing silicon and iron parts was used. The area ratio of the Fe and Si parts was varied. The deposition was carried out in the atmosphere of argon and oxygen. In the process of ion-plasma sputtering during the deposition of the $SiO_x\&Fe_yO_z(Fe)$ film, Ar ions knock out atoms from the combined silicon-iron target. The silicon and iron atoms are oxidized during their movement in the direction of the substrate, and the degree of oxidation depends on the ratio of oxygen and argon gases supplied to the chamber during the sputtering process.

The area ratio of the iron and silicon parts of the combined target was changed to obtain films with different iron and silicon contents. The area was fixed in the following ratios: Fe:Si = 2:1; Fe:Si = 1:1; Fe:Si = 1:2. Also, $Fe_yO_z(Fe)$ (Fe:Si = 1:0) and SiO_x (Fe:Si = 0:1) films were deposited as the edge cases of $SiO_x\&Fe_yO_z(Fe)$ compositions.

The oxygen content in the gas environment during deposition remained unchanged at 18%. The films were deposited on *p*-type (100) silicon substrates (ρ = 10 Ω·cm). The deposition was carried out in a vacuum chamber at P = $6.7\cdot10^{-3}\ldots1\cdot10^{-2}$ Pa, the substrate temperature T = 100…120 °C. The characteristics of the obtained experimental samples are given in Table. The atomic content in the films was determined using energy-dispersive X-ray spectroscopy.

After the film deposition, Al electrodes were formed on their surface using sputtering through the mask during thermal evaporation. The area of the metal electrodes was $7.85\cdot10^{-3}$ cm^2. Thus, MIS structures with the nanocomposite film as the dielectric were formed.

The measurements of the dielectric properties of $SiO_x\&Fe_yO_z(Fe)$ films were carried out using the Agilent 4249A semiconductor parameter analyzer within the range 5 kHz…5 MHz. To calculate the dielectric constant (ε') and dielectric loss (ε''), the parallel capacitance and dissipation factor were measured simultaneously.

Table. Characteristics of $SiO_x\&Fe_yO_z(Fe)$ films with different ratios of Fe and Si.

Ratio of target areas, Fe:Si	Atomic content in the film, at.%		
	Fe	Si	O
2:1	13.98	9.08	76.90
1:1	11.27	33.58	55.15
1:2	7.99	41.40	50.61
1:0	29.56	0	70.44
0:1	0	59.86	40.14

The analysis of dielectric losses was carried out by applying the MIS structure to the region with an accumulation of the major carriers in the near-surface layer of the semiconductor to eliminate the substrate influence.

3. Results and discussion

The dielectric loss tangent tg(δ) characterizes the dissipation of electromagnetic energy and its conversion into thermal energy. It is expressed as the ratio of the dielectric loss factor (the imaginary part of the dielectric permittivity ε'') to the dielectric constant (the real part of the dielectric permittivity ε'):

$$\tan(\delta) = \tan(90 - \phi) = \frac{\varepsilon''}{\varepsilon'}, \qquad (1)$$

where φ is the phase shift between the voltage and current.

The dielectric constant determines the part of incident electromagnetic energy on a material that is absorbed (stored and potentially released back), while the dielectric loss factor defines the portion of energy dissipated as heat within the material. The value of dielectric losses and its dependence on frequency, voltage, and temperature are governed by polarization mechanisms, including electronic polarization, ionic polarization, dipole polarization, and space charge polarization in heterogeneous materials (Maxwell–Wagner polarization) [28, 29]. In the case of quasi-elastic polarization, the dependence $\varepsilon_r(\omega)$ exhibits a resonant nature, with maxima and minima in $\varepsilon'(\omega)$. In contrast, the thermal polarization results in a relaxation-type dependence $\varepsilon_r(\omega)$, characterized by the gradual decrease in $\varepsilon'(\omega)$ with increasing frequency.

The dependences of the dielectric loss tangent on the voltage for the structures with initial (non-annealed) and annealed at T = 1000 °C $SiO_x\&Fe_yO_z(Fe)$ films are presented in Figs 1 and 2, respectively. The frequency dependences of dielectric losses at a fixed voltage U = –5 V for both initial and annealed nanocomposite films are shown in Figs. 3 and 4, respectively.

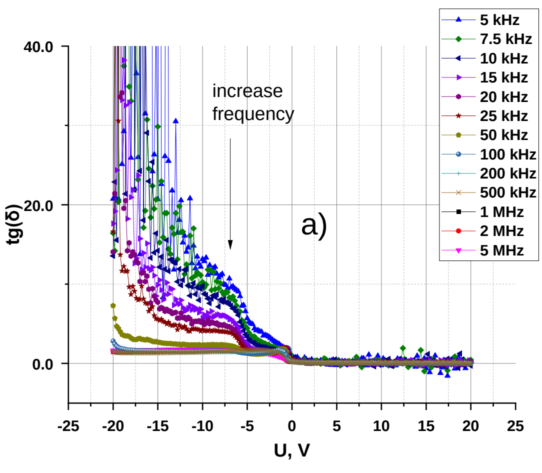

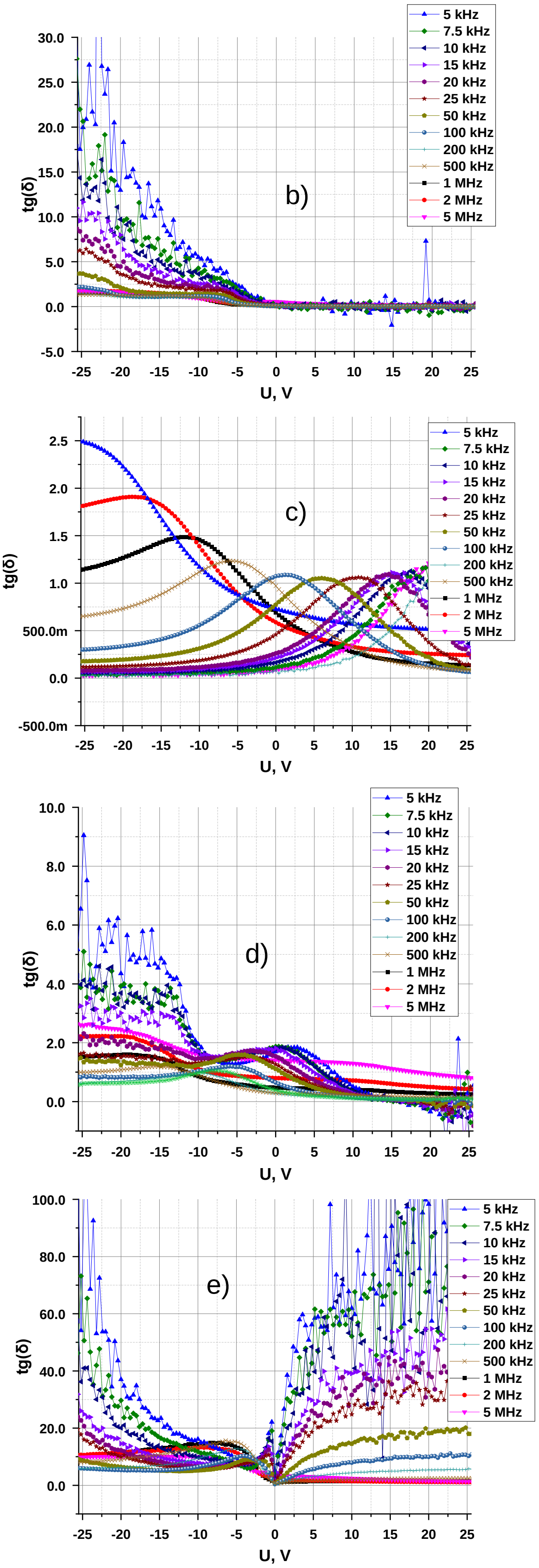

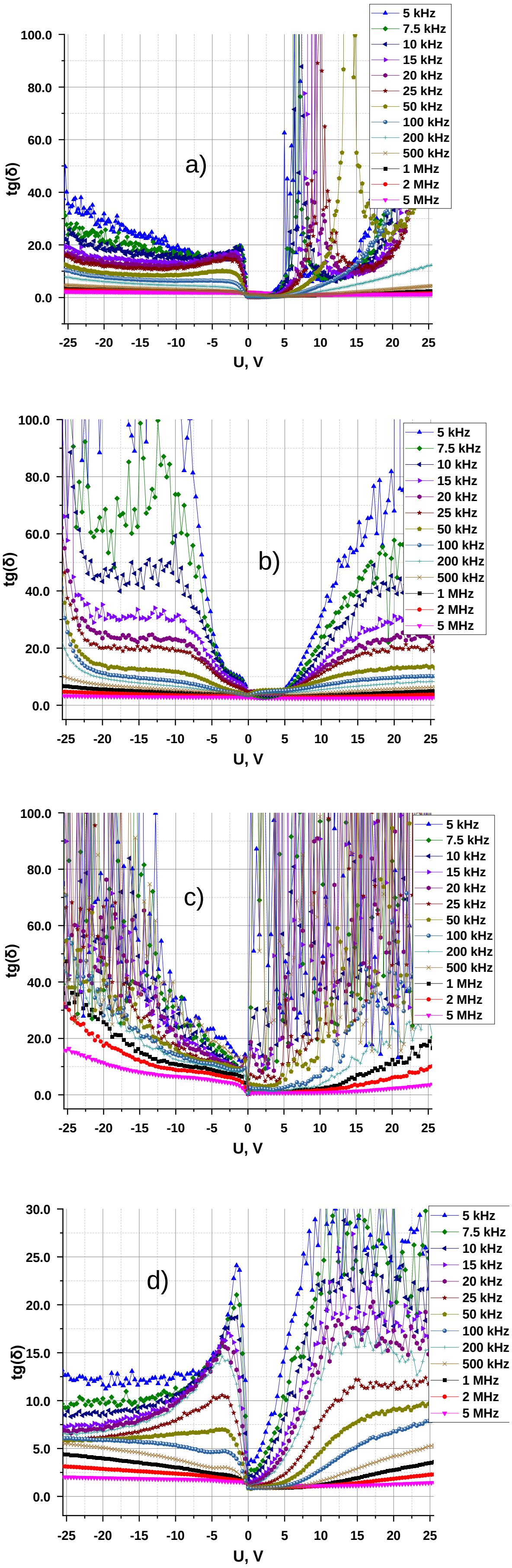

Fig. 1. Dependences of the dielectric loss tangent on the voltage for MIS structures with the initial nanocomposite films SiO_x&Fe_yO_z(Fe) as the dielectric: a) Fe:Si = 0:1, b) Fe:Si = 1:2, c) Fe:Si = 1:1, d) Fe:Si = 2:1, e) Fe:Si = 1:0.

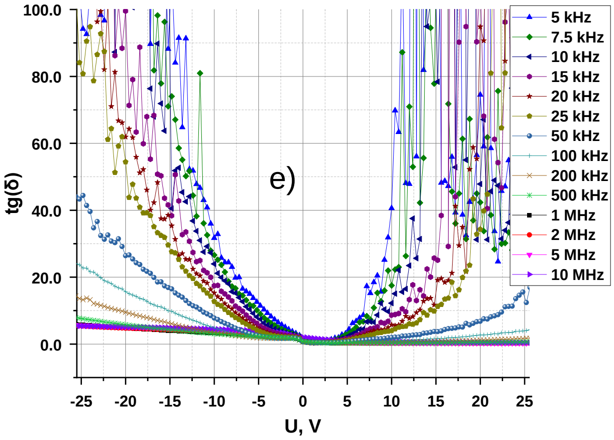

Fig. 2. Dependences of the dielectric loss tangent on the voltage for MIS structures with the thermally annealed (T = 1000 °C) nanocomposite SiO_x&Fe_yO_z(Fe) films as the dielectric: a) Fe:Si = 0:1, b) Fe:Si = 1:2, c) Fe:Si = 1:1, d) Fe:Si = 2:1, e) Fe:Si = 1:0.

In SiO_x&Fe_yO_z(Fe) films, the charge polarization at phase boundaries plays a significant role. An important mechanism of dielectric losses is the charge carrier scattering in the material, *i.e.*, losses due to electrical conductivity. The charge carrier scattering is caused by collisions with atoms and molecules in disordered (amorphous) materials, as well as by their interaction with phonons, impurities, and structural defects in crystals.

The studied SiO_x&Fe_yO_z(Fe) nanocomposite films contain numerous phase boundaries (Fe-Fe_yO_z, Fe_yO_z-SiO_x, SiO_x-Si), making charge polarization at interfaces (Maxwell–Wagner polarization) a crucial mechanism of dielectric losses. At the same time, these nanocomposite films exhibit noticeable electrical conductivity, indicating the significant contribution of electron scattering on atoms to dielectric losses. As a result, the intensity of atomic chaotic motion in the material increases, leading to a rise in dielectric temperature. In this case [28, 29]:

$$\tan\delta(\omega) = \frac{\sigma}{\varepsilon_0 \varepsilon_r \omega}, \qquad (2)$$

where σ is the electrical conductivity.

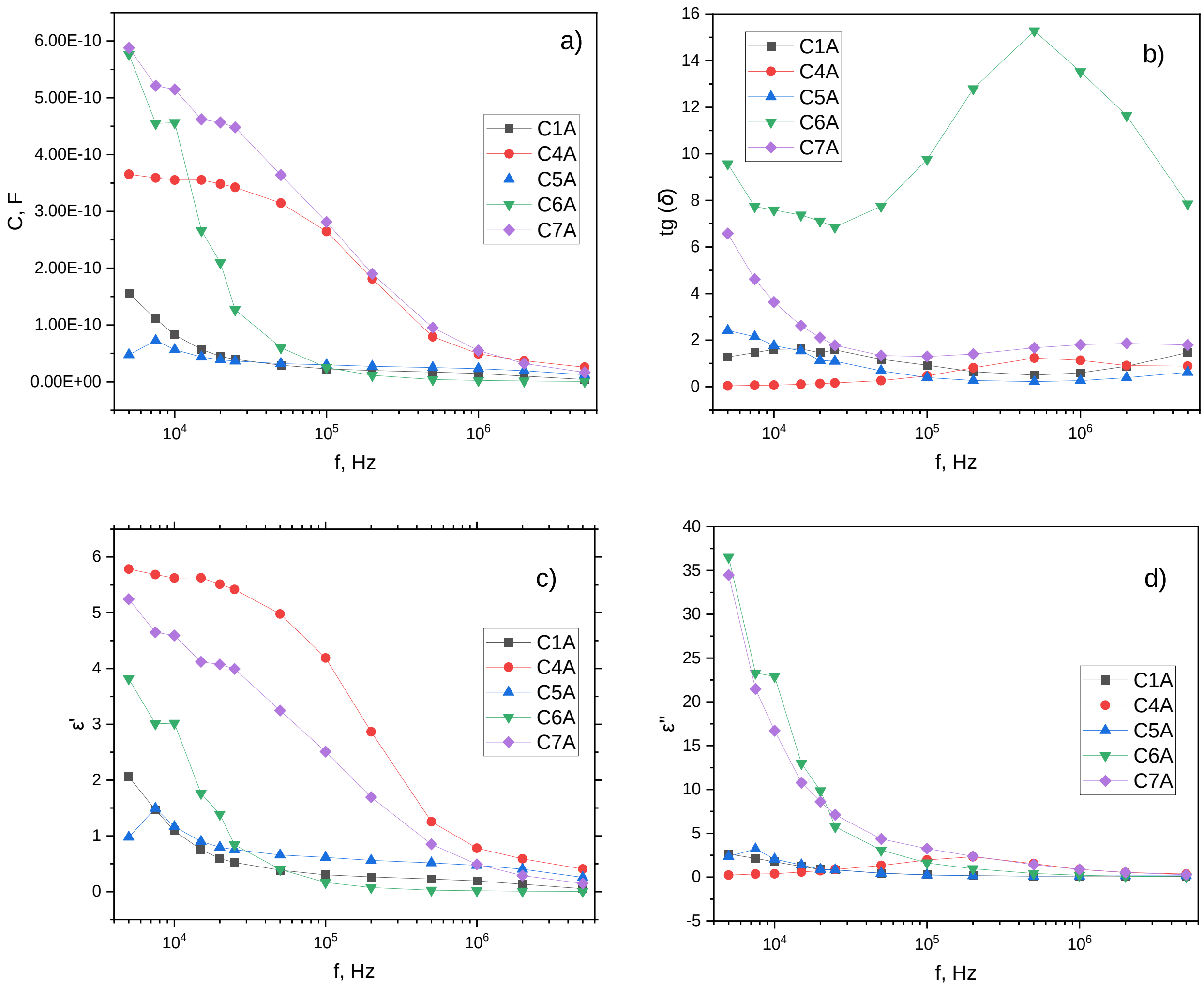

Fig. 3. Frequency dependences of the capacitance (a), dielectric loss tangent (b), dielectric constant (c) and dielectric loss factor (d) for the initial nanocomposite SiO_x&Fe_yO_z(Fe) films.

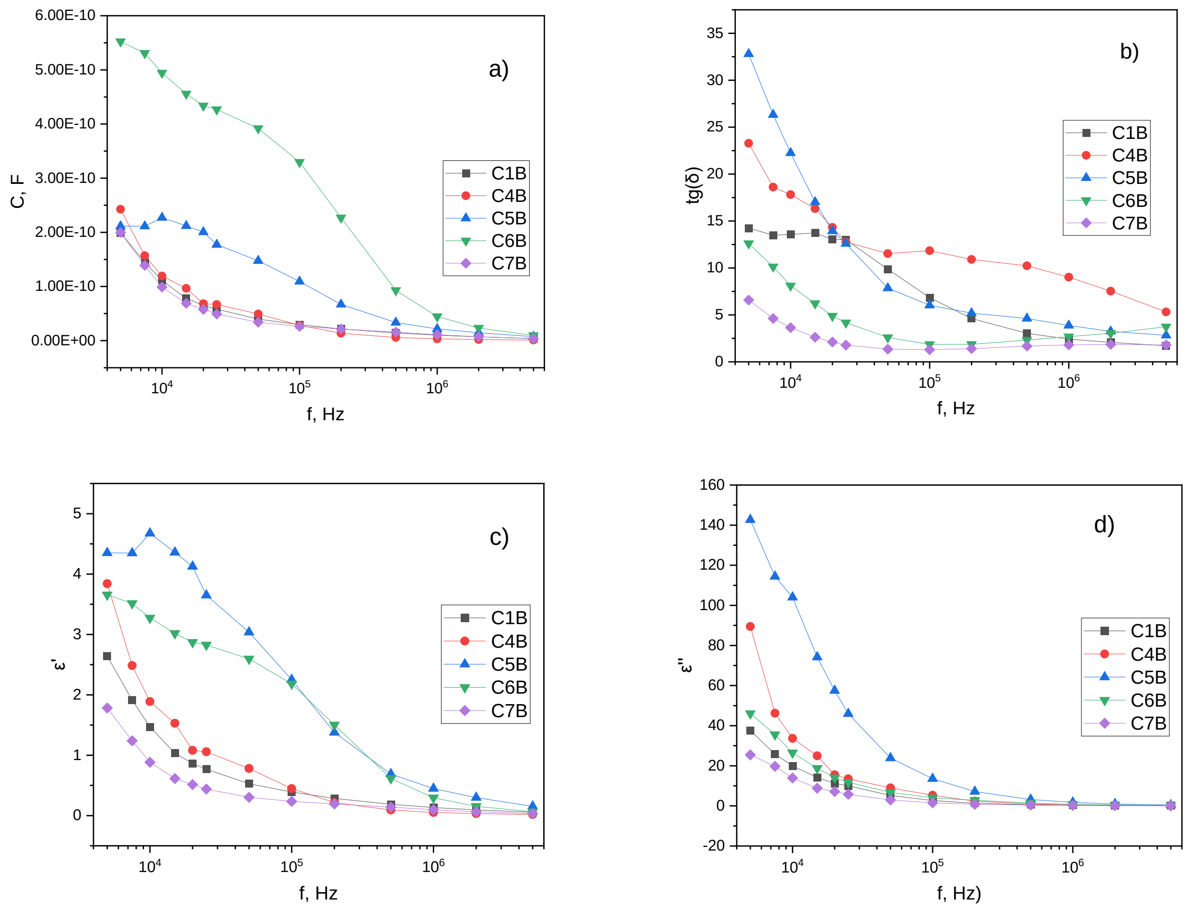

Fig. 4. Frequency dependences of the capacitance (a), dielectric loss tangent (b), dielectric constant (c), and dielectric loss factor (d) for the annealed nanocomposite SiO_x&Fe_yO_z(Fe) films.

One can see from expression (2) that the dielectric loss tangent tg(δ) increases with rising electrical conductivity and decreases with increasing frequency. It means that the material electrical conductivity enhances the dielectric loss factor ε″, the dielectric loss tangent tg(δ), and the dissipated energy within the material. The increase in voltage leads to the corresponding rise in the electric current, which in turn causes the increase in tg(δ), see Figs. 1 and 2.

At the same time, a significant decrease in tg(δ) with increasing frequency (Figs 1 and 3b) is observed. For SiO_x films (Fe:Si = 0:1) and SiO_x&Fe_yO_z(Fe) film with a low iron content (Fe:Si = 1:2), the dependences tg(δ)= $f(U)$ are monotonic, indicating that charge carrier scattering is the dominant mechanism of dielectric losses. However, increasing the iron content in nanocomposite SiO_x&Fe_yO_z(Fe) films (Fe/Si = 1:1, 2:1, 1:0) results in the non-monotonic dependence of tg(δ)= $f(U)$. This behavior suggests the involvement of the additional dielectric loss mechanisms, namely charge polarization at phase boundaries. High dielectric losses (tan (δ)) are observed for SiO_x&Fe_yO_z(Fe) films with Fe:Si = 0:1 (SiO_x), 1:2, and 1:0 (Fe_yO_z).

Dielectric losses in thermally annealed at T = 1000 °C SiO_x&Fe_yO_z(Fe) films also increase with increasing voltage and decrease with increasing frequency (Figs. 2 and 4b). They were significantly increased compared to the initial films. The most pronounced increase in tg(δ) after thermal annealing occurs in SiO_x&Fe_yO_z(Fe) films with Fe:Si = 1:1.

This increase in the dielectric losses after annealing is attributed to the phase separation in nanocomposite films, which enhances the dielectric loss mechanisms, namely charge polarization in phase boundaries and charge carrier scattering (*i.e.*, increased electrical conductivity). The increase in the conductivity after thermal annealing is confirmed by the DC current-voltage characteristic [30].

The frequency dependences of the capacitance, dielectric loss tangent, dielectric constant (ε′) and dielectric loss factor (ε″) for the initial and annealed nanocomposite SiO_x&Fe_yO_z(Fe) films are presented in Figs. 3 and 4, respectively. The dielectric constants (ε′) were calculated from the capacitance measurements and the dielectric loss factor (ε″) from the dielectric loss tangent using Eq. (1).

One can see in Figs. 3 and 4, tg(δ), ε′, and ε″, in general, decrease with increasing frequency. Only the initial film with the Fe:Si = 1:0 (Fe_yO_z) demonstrates the non-monotonic frequency dependence. This effect can be caused by magnetic resonances [29]. The highest dielectric losses are observed in this film. After thermal annealing, the dielectric losses increase for all films. For low frequencies, the dielectric losses are the highest for the films with Fe:Si = 1:2, but at higher frequencies – for the films with Fe:Si = 1:1. The increase in dielectric losses after thermal annealing is caused by the phase separation in SiO_x&Fe_yO_z(Fe) film and, as a result, due to formation of addition interfaces between phases. The growth of the interfaces promotes the enhancement of the important mechanism of dielectric losses, namely the space charge polarization in heterogeneous materials (Maxwell–Wagner polarization).

4. Conclusions

The dielectric losses in nanocomposite SiO_x&Fe_yO_z(Fe) films were investigated within 5 kHz…5 MHz. The SiO_x&Fe_yO_z(Fe) films with various fractions of iron and silicon were deposited using the ion-plasma sputtering method. The combined iron-silicon target with the possibility to change the areas of iron and silicon parts has been used. The SiO_x and Fe_yO_z films were also deposited as the edge cases of SiO_x&Fe_yO_z(Fe) films. The influence of the Fe/Si ratio in nanocomposite films on dielectric losses has been demonstrated. The frequency and voltage dependences of dielectric losses have been determined. Based on the obtained results we can summarize the following: 1) dielectric losses increase with increasing voltage; 2) dielectric losses decrease with increasing frequency; 3) dielectric losses depend on the Fe/Si ratio; 4) thermal annealing leads to the increase in dielectric losses; 5) for the initial films, the highest dielectric losses are observed at Fe:Si ratios equal to 1:0 (Fe_yO_z); 6) after thermal annealing, the highest dielectric losses are revealed in the films with Fe:Si ratios equal to 1:2 and 1:1. The peculiarities of dielectric losses in nano-composite SiO_x&Fe_yO_z(Fe) films were explained using the phenomenon of space charge polarization in phase interfaces.

Acknowledgements

This research was supported by the project "Development of nanocomposite material technology for highly efficient absorption of electromagnetic radiation" of the National Research Foundation of Ukraine (No. 2022.01/0066).

References

1. Abitbol M.H., Ahmed Z., Barron D. *et al*. *CMB-S4 Technology Book*, First Edition. 2017. https://doi.org/10.48550/arXiv.1706.02464
2. Hailey-Dunsheath S., Shirokoff E., Barry P.S. *et al*. Status of SuperSpec: a broadband, on-chip millimeter-wave spectrometer. *Proc. SPIE*. 2014. **9153**. id. 91530M (16 pp.). https://doi.org/10.1117/12.2057229.
3. Pan Z., Barry P.S., Cecil T. *et al*. Measurement of dielectric loss in silicon nitride at centimeter and millimeter wavelengths. *IEEE Trans. Appl. Superconduct*. 2023. **33**, No 5. Art No 1101707. https://doi.org/10.1109/TASC.2023.3264953.
4. Ye Z., Fülöp A., Helgason Ó.B. *et al*. Low-loss high-Q silicon-rich silicon nitride microresonators for Kerr nonlinear optics. *Opt. Lett*. 2019. **44**, No 13. P. 3326. https://doi.org/10.1364/OL.44.003326.
5. Paik H., and Osborn K. D. Reducing quantum-regime dielectric loss of silicon nitride for superconducting quantum circuits, *Appl. Phys. Lett.*, 2010. **96**, No. 7. https://doi.org/10.1063/1.3309703.
6. Defrance F., Shu S., Beyer A. *et al*. Low intrinsic TLS loss hydrogenated amorphous silicon. Millimeter, Submillimeter, and Far-Infrared Detectors and Instrumentation for Astronomy XI. *SPIE*. 2022. P. PC121900D. https://doi.org/10.48550/arXiv.2412.09693.
7. Buijtendorp B.T., Vollebregt S., Karatsu K. *et al*. Hydrogenated amorphous silicon carbide: A low-loss deposited dielectric for microwave to submillimeter wave superconducting circuits. *Phys. Rev. Appl*. 2022. **18**, No 6. P. 064003. https://doi.org/10.1103/PhysRevApplied.18.064003v
8. Samanta S., Maity A., Chatterjee S. *et al*. Rice–Bernasconi Gorkov–Eliashberg effect of giant dielectric permittivity in silica-based films containing interrupted silver nanowires. *Trans. Indian Inst. Met*. 2019. **72**, No 8. P. 1963–1969. https://doi.org/10.1007/s12666-018-1524-4.
9. Maity A., Samanta S., Roy S. *et al*. Giant dielectric constant of copper nanowires/amorphous SiO_2 composite thin films for supercapacitor application. *ACS Omega*. 2020. **5**, No 21. P. 12421–12430. https://doi.org/10.1021/acsomega.0c01186.
10. Evtukh A.A., Kizjak A.Yu., Bratus O.L. Impedance of nanocomposite SiO_2(Si)&Fe_xO_y(Fe) thin films containing Si and Fe nanoinclusions. *SPQEO*. 2023. **26**. P. 424–431. https://doi.org/10.15407/spqeo26.04.424.
11. Kizjak A.Yu., Evtukh A.A., Bratus O.L. *et al*. Electron transport through composite SiO_2(Si)&Fe_xO_y(Fe) thin films containing Si and Fe nanoclusters. *J. Alloys Compd*. 2022. **903**. P. 163892. https://doi.org/10.1016/j.jallcom.2022.163892.
12. Ilchenko V.V., Marin V.V., Vasyliev I.S. *et al*. Admittance spectroscopy using for the determination of parameters of Si nanoclusters embedded in SiO_2. *2014 IEEE 34th Int. Sci. Conf. on Electronics and Nanotechnology (ELNANO)*, 2014. P. 86–89. https://doi.org/10.1109/ELNANO.2014.6873969.
13. Evtukh A., Bratus' O., Ilchenko V. *et al*. Capacitive properties of MIS structures with SiO_x&$Si_xO_yN_z$ films containing Si nanoclusters. *J. Nano Res.* 2016. **39**. P. 162–168. https://doi.org/10.4028/www.scientific.net/JNanoR.39.162.
14. Zhang D., Wang R., Wen M. *et al*. Synthesis of ultralong copper nanowires for high-performance transparent electrodes. *J. Am. Chem. Soc.* 2012. **134**, No 35. P. 14283–14286. https://doi.org/10.1021/ja3050184.

15. Bhattacharjee S., Banerjee A., Mazumder N. *et al*. Negative capacitance switching in size-modulated Fe_3O_4 nanoparticles with spontaneous non-stoichiometry: Confronting its generalized origin in non-ferroelectric materials. *Nanoscale*. 2020. **12**, No 3. P. 1528–1540. https://doi.org/10.1039/C9NR07902E.
16. Parravicini G.B., Stella A., Ungureanu M.C., Kofman R. Low-frequency negative capacitance effect in systems of metallic nanoparticles embedded in dielectric matrix. *Appl. Phys. Lett.* 2004. **85**, No 2. P. 302–304. https://doi.org/10.1063/1.1772872.
17. Evtukh A., Kizjak A., Bratus O. *et al*. Negative capacitance and dielectric constant of nanocomposite $SiAl_zO_xN_y$ (Si) films with semiconductor nanoparticles. *Nano Lett*. 2024. **24**, No 2. P. 617–622. https://doi.org/10.1021/acs.nanolett.3c03627.
18. Elmahaishi M.F., Azis R.S., Ismail I., Muhammad F.D. A review on electromagnetic microwave absorption properties: their materials and performance. *J. Mater. Res. Technol*. 2022. **20**. P. 2188–2220. https://doi.org/10.1016/j.jmrt.2022.07.140.
19. Zhang Y., Zhang Y., Li Y. *et al*. Facile design and permittivity control of reduced graphene oxide foam/TiO_2 3D composite towards lightweight and high-efficient microwave absorption. *J. Alloys Compd*. 2021. **889**. P. 161695. https://doi.org/10.1016/j.jallcom.2021.161695.
20. Liang H., Xing H., Qin M., Wu H. Bamboo-like short carbon fibers@Fe3O4@phenolic resin and honeycomb-like short carbon fibers@Fe_3O_4@FeO composites as high-performance electromagnetic wave absorbing materials. *Compos. A: Appl. Sci. Manuf.* 2020. **135**. P. 105959. https://doi.org/10.1016/j.compositesa.2020.105959.
21. Lu Y., Yin Y., Mayers B.T., Xia Y. Modifying the surface properties of superparamagnetic iron oxide nanoparticles through a sol–gel approach. *Nano Lett*. 2002. **2**, No 3. P. 183–186. https://doi.org/10.1021/nl015681q.
22. Santra S., Tapec R., Theodoropoulou N. *et al*. Synthesis and characterization of silica-coated iron oxide nanoparticles in microemulsion: The effect of nonionic surfactants. *Langmuir*. 2001. 17, No 10. P. 2900–2906. https://doi.org/10.1021/la0008636.
23. Tartaj P., Serna C.J. Synthesis of monodisperse superparamagnetic Fe/silica nanospherical composites. *J. Am. Chem. Soc*. 2003. **125**, No 51. P. 15754–15755. https://doi.org/10.1021/ja0380594.
24. Ebrahimi-Tazangi F., Hekmatara S.H., Seyed-Yazdi J. Remarkable microwave absorption of GO-SiO_2/Fe_3O_4 via an effective design and optimized composition. *J. Alloys Compd*. 2021. **854**. P. 157213. https://doi.org/10.1016/j.jallcom.2020.157213.
25. Jaiswal R., Agarwal K., Pratap V. *et al*. Microwave-assisted preparation of magnetic ternary core-shell nanofiller ($CoFe_2O_4$/rGO/SiO_2) and their epoxy nanocomposite for microwave absorption properties. *Mater. Sci. Eng.: B*. 2020. **262**. P. 114711. https://doi.org/10.1016/j.mseb.2020.114711.
26. Kelsall R.W., Hamley I.W., Geoghegan M. (Eds). *Nanoscale Science and Technology*, 1st ed. Wiley, 2005. https://doi.org/10.1002/0470020873.
27. Bratus O.L. Structural properties of nanocomposite SiO_2(Si) films obtained by ion-plasma sputtering and thermal annealing. *SPQEO*. 2011. **14**. P. 247–255. https://doi.org/10.15407/spqeo14.02.247.
28. Poplavko Yu.M. *Electronic Materials: Principles and Applied Science*. Elsevier, Amsterdam, 2019.
29. Javid M., Zhou Y., Wang D. *et al*. Magnetic behavior, electromagnetic multiresonances, and microwave absorption of the interfacial engineered Fe@FeSi/SiO_2 nanocomposite. *ACS Appl. Nano Mater*. 2018. **1**, No 3. P. 1309–1320. https://doi.org/10.1021/acsanm.8b00055.
30. Bratus O., Kizjak A., Kykot A. *et al*. Influence of the annealing temperature on the electrical conductivity mechanisms SiO_x(Si)&Fe_yO_z(Fe) films. *J. Alloys Compd*. 2025. **1011**. P. 178383. https://doi.org/10.1016/j.jallcom.2024.178383.

Authors' contributions

Evtukh A.A.: key ideas, conceptualization, analysis, validation, supervision, writing – review & editing.
Antonin S.V.: measurements, investigations, analysis, discussion, writing – review & editing.
Pypypov A.I.: initial draft preparation, writing.
Bratus O.L.: film deposition, investigations, conceptualization.

Authors and CV

Anatoliy Evtukh, Doctor of Sciences, Professor, Leading Researcher at the Department of Physics of Surface and Nanophotonics, V. Lashkaryov Institute of Semiconductor Physics, NAS of Ukraine. Authored over 300 publications. His main research activity is in the field of nanomaterials and nanostructures, composite films with semiconductor and metal nanoinclusions, electron transport, surface physics, semiconductor technologies, sensors and solar cells.
E-mail: anatoliy.evtukh@gmail.com,
https://orcid.org/0000-0003-3527-9585

Serhii Antonin was born in 1994, defended his PhD thesis in applied physics and nanomaterials in 2022. Junior researcher at the V. Lashkaryov Institute of Semiconductor Physics, NAS of Ukraine. The area of scientific includes nanomaterials and nanostructures, composite films, semiconductor technologies and solar cells.
https://orcid.org/0000-0003-1607-9721

Pylypov Anton, PhD student at the Taras Shevchenko National University of Kyiv, Educational and Research Institute of High Technologies, was born in 1988. He defended his master thesis in 2010 at the National Mining University, Department of electricity system. The area of his scientific interests includes physics and technology of semiconductor materials, electronics devices and sensors (photoresistors, light-emitted structures *etc*.), as well as the analysis, diagnostics, modeling and forecasting of physical processes in different objects, knowledge of circuitry, electronics and modern element base. E-mail: pylypov.anton@gmail.com, https://orcid.org/0009-0009-2996-1503

Oleh Bratus, PhD in Physics and Mathematics (Physics of Solid States), Senior Researcher at the Department of Physics of Surface and Nanophotonics, V. Lashkaryov Institute of Semiconductor Physics, NAS of Ukraine. Authored over 80 publications. His main research activity is in the field of semiconductor technologies, nanomaterials and nanostructures, composite films with semiconductor and metal nanoinclusions, electron transport, surface physics, and solar cells.
E-mail: o.l.bratus@gmail.com,
https://orcid.org/0000-0002-2661-6482

Діелектричні втрати в нанокомпозитних плівках SiO_x&Fe_yO_z(Fe)

А.А. Євтух, С.В. Антонін, А.І. Пилипов, О.Л. Братусь

Анотація. Дослідження діелектричної поведінки нанокомпозитних плівок дуже важливі для кращого розуміння поглинання електромагнітних хвиль. У цій роботі представлено результати дослідження діелектричних втрат у нанокомпозитних плівках SiO_x&Fe_yO_z(Fe). Плівки різного складу отримано методом фізичного іонно-плазмового напилення. Досліджено діелектричні втрати в діапазоні частот 5 кГц – 5 МГц Продемонстровано зменшення діелектричних втрат із збільшенням частоти та їх збільшення з ростом напруги прикладеного сигналу. Вміст нанокомпозитних плівок SiO_x&Fe_yO_z(Fe) та їх високотемпературний відпал істотно впливають на діелектричні втрати. Найбільші діелектричні втрати спостерігаються для вихідних плівок Fe_yO_z. Але у випадку відпалених плівок найбільші діелектричні втрати були для плівок із співвідношенням площ мішеней для розпилення Fe:Si = 1:2 та 1:1. Результати пояснено на основі явища поляризації просторового заряду на межах поділу фаз.

Ключові слова: нанокомпозитні плівки, діелектричні втрати, поляризація, частота, напруга, іонно-плазмове осадження, відпал.